JOURNAL OF ENVIRONMENTAL SCIENCES 155 (2025) 832–845

Available online at www.sciencedirect.com

ScienceDirect

www.elsevier.com/locate/jes

JES JOURNAL OF ENVIRONMENTAL SCIENCES

www.jesc.ac.cn

Research Article

Suitability of using carbon dioxide as a tracer gas for studying vehicle emission dispersion in a real street canyon

Yuhan Huang[1,*], *Helen B. Wang*[2,*], *Hilda M.W. Mak*[2], *Mengyuan Chu*[3], *Zhi Ning*[3], *Bruce Organ*[4], *Edward F.C. Chan*[2], *Chun-Ho Liu*[5], *Wai-Chuen Mok*[5], *Christof Gromke*[6], *Ho Kyong Shon*[1], *Chengwang Lei*[7], *John L. Zhou*[1]

[1] *Centre for Green Technology, School of Civil and Environmental Engineering, University of Technology Sydney, NSW, 2007, Australia*
[2] *Faculty of Science and Technology, Technological and Higher Education Institute of Hong Kong, Hong Kong, China*
[3] *Division of Environment and Sustainability, The Hong Kong University of Science and Technology, Hong Kong, China*
[4] *Jockey Club Heavy Vehicle Emissions Testing and Research Centre, Vocational Training Council, Hong Kong, China*
[5] *Department of Mechanical Engineering, The University of Hong Kong, Hong Kong, China*
[6] *Laboratory of Building and Environmental Aerodynamics, Institute for Water and Environment, Karlsruhe Institute of Technology, Karlsruhe, Germany*
[7] *Centre for Wind, Waves and Water, School of Civil Engineering, The University of Sydney, NSW, 2006, Australia*

ARTICLE INFO

Article history:
Received 30 October 2023
Revised 23 June 2024
Accepted 25 June 2024
Available online 4 July 2024

Keywords:
Vehicle emission dispersion
Tracer gas
Carbon dioxide
Urban street canyon
Line emission source
Point emission source

ABSTRACT

High-rise buildings form deep urban street canyons and restrict the dispersion of vehicle emissions, posing severe health risks to the public by aggravating roadside air quality. Field measurements are important for understanding the dispersion process of tailpipe emissions in street canyons, while a major challenge is the lack of a suitable tracer gas. Carbon dioxide (CO_2), which is safe to the public and inexpensive to obtain, can be reliably measured by existing gas analysers. This study investigated the suitability of using CO_2 as a tracer gas for characterising vehicle emission dispersion in a real-world street canyon. The tracer gas was released via a line or point source, whose dispersion was characterised by a sensors network comprising low-cost air quality sensors. The results showed that the CO_2 contained in the exhaust gas of a test vehicle itself had unmeasurable effect at roadsides. Both the line and point sources produced obvious CO_2 level elevations at approximately 30 s after the test vehicle passed by. In addition, for both line and point sources, the CO_2 elevations were much more distinct at the roadside next to tailpipe exit than the opposite side, and were higher at 0.8 m than 1.6 m above the ground. The present study demonstrated that using CO_2 as a tracer gas is feasible for investigating vehicle emission dispersion in

* Corresponding authors.
E-mails: yuhan.huang@uts.edu.au (Y. Huang), beiwang@vtc.edu.hk (H.B. Wang).

https://doi.org/10.1016/j.jes.2024.06.036

real-world street canyons. Future studies are needed to improve the gas release rate of the developed tracer gas systems for more reliable measurements and larger street canyons.

Introduction

Ambient air pollution at both street and regional levels remains a serious environmental problem in Hong Kong (Cheng et al., 2021; Hossain et al., 2021). The Hedley Environmental Index (2023) estimated that air pollution in Hong Kong caused 1329 premature deaths, 1.7 million doctor visits and HK$15.8 billion total economic losses in 2021. Roadside air pollution problem is usually more serious than background air pollution due to the proximity to emission sources (i.e., motor vehicles) and the reduced emission dispersion capability when urban street canyons are present (Huang et al., 2021; Pettit et al., 2021; Yang et al., 2020). The Hong Kong air quality monitoring network data showed that the annual average nitrogen dioxide (NO_2) concentrations measured at roadside stations were much higher (e.g., 45 %–210 % higher in 2018) than those at background stations (Huang et al., 2020b). Similar roadside air pollution problems were also widely observed in many other cities globally (Casquero-Vera et al., 2019; Grange et al., 2017; Takekawa et al., 2013; Wu et al., 2022). This poses a severe health risk to the public, considering that urban streets are important communal places for city inhabitants nowadays (Alexeeff et al., 2018; Huang et al., 2022; Rivas et al., 2019).

Developed countries predominantly adopt low development density and hence are less affected by roadside air pollution aggravated by urban street canyons. However, land scarcity has made tall and dense buildings a typical feature of Hong Kong's cityscape (Kwok et al., 2021; Zheng et al., 2018), leading to the formation of many urban street canyons with high aspect ratios of building height over street width. Insufficient understanding of the pollutant dispersion process limits our capability to evaluate the effectiveness of control measures and the implications of city development projects for roadside air quality (Lee, 2019; Li and Zhou, 2019; Zhou and Lin, 2019).

Field measurements are essential for understanding the dispersion process of tailpipe emissions in urban street canyons. A proper tracer gas is the key for dispersion experiments (Mendes et al., 2015; Simmonds et al., 2021). According to Laporthe et al. (2001), an ideal tracer gas should possess a number of characteristics, including: 1) no harm to people, materials or activities in the experimental area, 2) not inflammable, toxic or explosive, 3) no chemical/physical reactions, absorptions or decompositions in the environment, 4) similar molecular weight to that of air, 5) no interference/impacts on the studied process or air movement, 6) absent in air, and 7) amenable to accurate detection at low concentrations. Unfortunately, no tracer gas can fully meet all the above criteria and some additional considerations are necessary when choosing a tracer gas, such as gas cost and measurement equipment (Laporthe et al., 2001).

Sulphur hexafluoride (SF_6) is odourless, non-toxic, inert and exotic to the environment, and can be reliably measured at very low concentrations (at ppb levels) (Connan et al., 2011; Guo et al., 2001; Xu et al., 2013). Therefore, SF_6 has been widely used as a tracer gas for air dispersion studies, in particular in laboratory wind tunnel investigations. Gromke et al. (2016) investigated the effect of roadside hedgerows on traffic pollutant dispersion in a reduced scale (1:150) street canyon model using a line source releasing SF_6 in a wind tunnel. They found that continuous hedgerows could effectively reduce street-level pollutant concentrations, especially in the most polluted centre area of a street canyon. Huang et al. (2020a) measured the thermal effect on dispersion of rooftop stack emissions in a step-down street canyon (scale of 1:100) using a point source emitting SF_6 in a wind tunnel. The results showed that the thermal effect on the downwind building roof increased emission dispersion to the upper urban boundary layer and thus reduced street-level air pollution. Zhang et al. (2022) measured and simulated the effect of an obstacle on the transport process of a dense gaseous contaminant (represented by SF_6) in a closed chamber. They revealed three transport modes (i.e., passive, transitional, and active) around the contaminant source, among which the active transport mode had the highest overall ventilation efficiency. Fu et al. (2022) developed a fast-response SF_6 measuring system based on a quartz-enhanced photoacoustic spectroscopy (QEPAS) and evaluated its performance against a conventional commercial instrument. The results showed that, while both instruments could obtain similar average concentrations, the QEPAS instrument successfully captured the rapidly changing SF_6 concentrations, but the conventional commercial instrument did not.

To date, very few studies have been carried out in real-world street canyons to characterise the dispersion process of vehicle emissions. SF_6 would not be a suitable tracer gas for such applications due to the following reasons. Firstly, real-world dispersion of vehicle emissions is highly dynamic, often changing within seconds, necessitating rapid measurements to capture the transient variations of tracer gas concentrations. However, the prevalent commercial SF_6 measurement instruments usually have long sampling durations and data acquisition intervals (up to 45 s) (Fu et al., 2022). Secondly, the density of SF_6 (6.17 kg/m^3) is much larger than those of air (1.23 kg/m^3) and vehicle emissions (e.g., 1.87 kg/m^3 for CO_2 and 1.14 kg/m^3 for CO), which would lead to different dispersion characteristics, especially when the flow field is laminar or of low turbulence, and thus would not represent the dispersion of vehicle emissions. Laporthe et al. (2001) compared the performance of two tracer gases, namely SF_6 (6.17 kg/m^3)

and N_2O (1.22 kg/m^3, practically the same density as that of air). Their experimental results showed that N_2O tended to mix and disperse more quickly than SF_6 due to its much lower density. Thirdly, SF_6 is the most potent greenhouse gas whose global warming potential is 23,500 times of CO_2 (Harrison, 2020; Li et al., 2019). This becomes especially concerning since field experiments would necessitate a much larger quantity of gas than wind tunnel experiments. Finally, SF_6 is costly.

In contrast, CO_2 is an odourless, inert, non-toxic and inexpensive gas with a density similar to that of air, whose measurements can be conducted at a much lower cost and higher frequency than SF_6. Therefore, CO_2 could be a suitable tracer gas for representing the dispersion process of vehicle emissions. The challenge, however, is to develop a CO_2 tracer gas system (including a measurement sensors network) that could study the dispersion process of tailpipe emissions in an urban street canyon in the presence of concurrent CO_2 emissions from vehicles in the study environment. CO_2 was deployed to simulate the dispersion of toxic heavy gases in street canyons using wind tunnel experiments and CFD modelling (Tan et al., 2019; 2018). However, to the best of the authors' knowledge, no experimental studies have used CO_2 as a tracer gas to investigate the dispersion process of vehicle emissions.

Accordingly, this paper aimed to examine the suitability of using CO_2 as a tracer gas for studying the dispersion process of tailpipe emissions in a real-world street canyon. A tracer gas system was developed to release CO_2 gas at a quantity sufficient to reveal the dispersion characteristics of the tailpipe emissions despite the interference from the CO_2 emissions of a test vehicle itself. To verify the adequacy of the developed tracer gas system, a novel test method of combining two emission measurement techniques, including a portable emission measurement system (PEMS) and a roadside emission sensor network (RESN) composed of low-cost small-size air quality sensors, was developed for characterising the CO_2 dispersion process, which provided a full picture from tailpipe to roadside.

1. Materials and methods

1.1. Test site and vehicle

Field experiments were carried out on a private road where the CO_2 emissions were from sources dedicated to the experiments, i.e., a CO_2 line/point source for simulating vehicle emissions on a road and a diesel test vehicle for generating turbulence as a result of vehicle movement, on top of a general background CO_2 level (i.e., ~400 ppm in this study) that was monitored during the experiments. The test site was a private road on the THEi Tsing Yi Campus (Fig. 1a), which has a 10-storey building of about 100-m length on one side and a steep hill several times taller than the building on the other side. The test vehicle was an IVECO EUROCARGO diesel medium goods vehicle (Fig. 1b), with a manufacture year of 2018, an engine displacement of 6728 cc, and a gross vehicle weight of 16 t. A set of PEMS was installed on the test vehicle to take comprehensive measurements at a frequency of 1 Hz, including the exhaust flow rate, exhaust temperature, emission concentration, vehicle speed, air humidity and air temperature. The exhaust tailpipe was pointing at the left rear wheel after the installation of the PEMS and the point source tracer gas system (Fig. 1b).

Fig. 1 – Experimental setup. (a) the test site; (b) the roadside emission sensors and the test vehicle equipped with PEMS.

1.2. Line source experiments

Fig. 2 shows the setup of the line source experiments. The CO_2 line source was placed on the building side at about 0.3 m from the RESN. It was a 20-m long steel reinforced polymer hose with an inner diameter of 1.0 inch (25.4 mm). CO_2 was released from holes that were 0.5-m equispaced along its length. The hole diameter was 5.00 mm in the first 10 m and was increased to 6.35 mm in the second 10 m. Further to this, some holes were partially blocked by tapes to ensure even release (spatially homogeneous) of the gas along the line source, which was checked by ambient air sensors at their respective measurement locations. Such checks were performed, and adjustments were made (if required) before each line source measurement series.

The line source was supplied by a 180-L liquid gas cylinder which had a nominal net weight of 175 kg, a gas purity level of 99.7 % and a maximum pressure of 25 bar. The line source and CO_2 cylinder were connected by another steel reinforced polymer hose with a length of 6 m and an inner diameter of 0.5 inch (12.7 mm). A high-flow high-purity Vigour VSR3ELC gas regulator was fitted to the gas bottle to ensure a constant gas supply. The gas flow was actuated with a manually controlled valve at the beginning of each line source test run. Due to the rapid cooling associated with phase change from liquid to gas CO_2, the regulator and valves were kept warm by hot air guns to avoid freezing the regulator or sealing components.

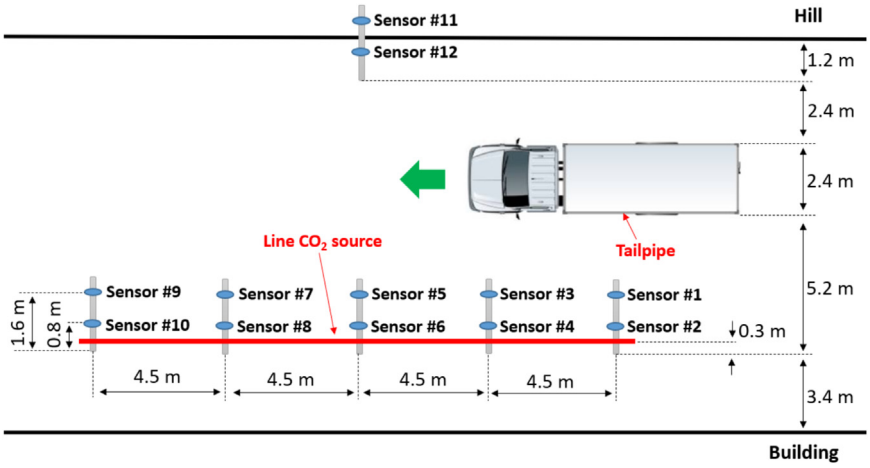

Fig. 2 – Setup of line emission source experiments.

The RESN was used to characterise the CO_2 dispersion process at both roadsides, which consisted of six pairs of low-cost small-size air quality sensors. The sensors used in the experiments are HKUST in-house sensors referred to as High Speed Sensors (HSS). HSS are small size (205 mm × 160 mm × 90 mm) and light weight (<1.15 kg), include pumps for active sampling, and cause negligible obstruction for CO_2 dispersion. The Premier Platinum Infrared High Power Dual Range CO_2 Sensor (Dynament, UK) was used for CO_2 measurements, which operates based on nondispersive infrared (NDIR) method. The sensor can measure a range of CO_2 from 0 to 5 % by volume (set as 1 % in this study), with a resolution of 10 ppm by volume and a response time of T_{50} < 10 s. The sensor is temperature compensated over the range of −20 °C to 50 °C. Gas concentrations and system status data were transmitted to a local server for real-time monitoring and stored locally in an SD card for backup. With a built-in pump and a battery, the HSS can operate continuously for more than 12 h. More information about the HSS can be found in our earlier works (Brimblecombe et al., 2021; Chu et al., 2022).

All sensors were calibrated at the beginning of the experiments. They sampled CO_2 concentrations at 1 Hz when the line source was switched on and/or the test vehicle passed by. Before experiments began, pilot trials with three pairs of sensors on each roadside were performed, which showed that the sensors on the hill side could not measure any obvious CO_2 changes. Therefore, only one pair of sensors was placed on the hill side and the rest five pairs of sensors were placed on the building side to capture CO_2 variations at a higher spatial resolution. Each pair of sensors was installed on a tripod with a 4.5 m spacing. The sensor heights represented two typical human breathing zones, i.e., 0.8 m for children and 1.6 m for adults (Fig. 2). In addition to the considerations of human breathing zones, the measurements at two different sensor heights are also very useful for developing and calibrating an urban canyon emission dispersion model in future studies.

The experiments were conducted under three scenarios (Table 1), including (1) test vehicle only, (2) line source only, and (3) test vehicle plus line source. In the test vehicle only scenario, the vehicle drove through the street canyon at three constant speeds of 5, 15 and 30 km/h, which served as the only CO_2 emission source. This was to investigate if the CO_2 gas exhausted from the test vehicle itself would cause any measurable CO_2 elevations at the roadsides in the studied canyon. In the line source only scenario, the line source was switched on for 20 s at two pressures of 24 and 12 bar, which released about 0.073 and 0.061 kg/s of CO_2 gas, respectively. In the test vehicle plus line source scenario, both the line source (24 and 12 bar) and test vehicle (5, 15 and 30 km/h) were used. The line source was switched on only when the vehicle passed through the canyon. This was to investigate the CO_2 dispersion process under the influence of turbulence induced by a moving vehicle.

Each experimental condition was repeated for at least three times. The RESN sensors recorded the CO_2 concentrations continuously at 1 Hz during the test day. The start and end times of each experiment were logged manually. The ambient conditions of temperature, humidity and wind were also recorded for each experiment. Table 1 also gives the ambient conditions during the experiments. The experiments were performed on a sunny day from 10.30am to 3.00pm. The ambient temperature and humidity were measured by the RESN sensors. The wind speed was measured by a TSI Airflow TA410 meter and the wind direction was measured by a compass. The ambient temperature and humidity were relatively stable at around 30 °C and 60 %, respectively, during the whole tests. In comparison, the wind speed was more dynamic between experiments (0.8–2.6 m/s, light air to light breeze). However, due to the presence of the steep hill next to the building and the stable prevailing wind direction on the measurement day in the Hong Kong region, the wind direction was unchanged during the experiments, which flowed against the vehicle driving direction (Fig. 2).

1.3. *Point source experiments*

Fig. 3 shows the setup of point source experiments. The point source CO_2 tracer gas system was installed inside the con-

Table 1 – Experimental and ambient conditions.

Experimental conditions		Wind speed (m/s)	Temperature (°C)	Humidity (%)
Scenario 1	Test vehicle only (30 km/h)	2.6	29	64
	Test vehicle only (15 km/h)	1.4	29	66
	Test vehicle only (5 km/h)	0.9	31	61
Scenario 2	Line source only (high rate)	0.8	29	66
	Line source only (low rate)	2.0	34	53
Scenario 3	30 km/h + line source (high rate)	1.9	30	62
	15 km/h + line source (high rate)	2.5	29	63
	5 km/h + line source (high rate)	2.6	29	66
	30 km/h + line source (low rate)	2.3	31	61
	15 km/h + line source (low rate)	1.6	32	58
	5 km/h + line source (low rate)	1.6	33	55

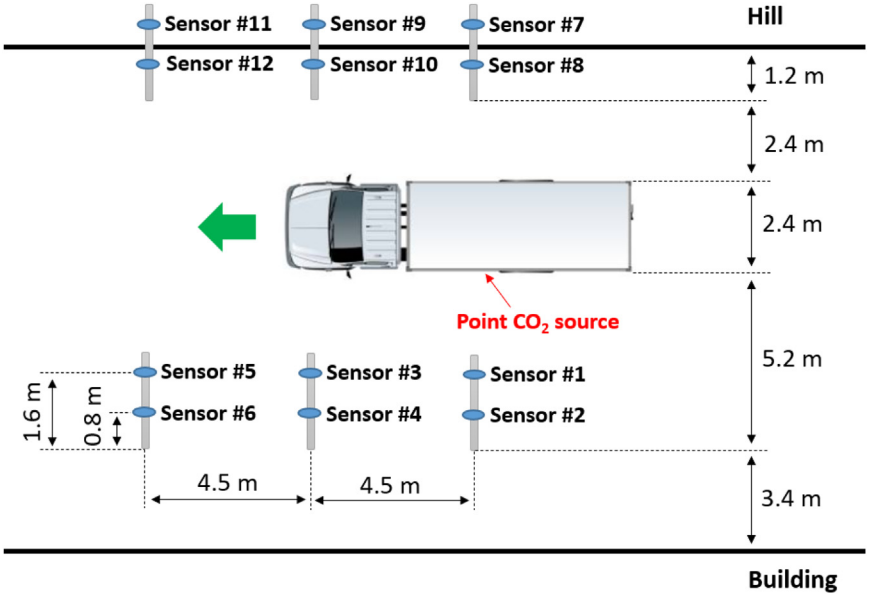

Fig. 3 – Setup of point emission source experiments.

tainer of the test vehicle, which injected pure CO_2 gas into the exhaust tailpipe. The same type of CO_2 cylinder employed with the line source was used for the point source tests. The gas regulator was also the same, but a remotely actuated gas valve was used to start and stop the gas flow. The actuator used was a Swagelok electric actuator (MS-142DC, 24 V DC) which was fitted onto the flow control valve. At the start of a test run, the operator sitting in the cabin of the truck started the flow from the gas cylinder and stopped the flow after passing the last gas sensors. A further difference was that a gas manifold was used to separate the gas flow after the valve into 4 separate tubes which delivered the gas to equispaced injection points on the exhaust adapter connected to the exhaust pipe of the test vehicle. At the source side, the tailpipe exhaust flow rates, emission concentrations and temperature were measured by the PEMS at 1 Hz. At the roadside, three pairs of air quality sensors were placed at each side of the road to form a RESN, which measured CO_2 concentrations at 1 Hz when the test vehicle passed by. Similar to the line source experiments, each pair of sensors was installed on a tripod with 4.5 m spacing, at two typical human breathing heights of 0.8 and 1.6 m above the ground. The experiments were conducted at 15 km/h driving speed under two conditions, i.e., with and without the tracer gas system. The ambient wind speeds were 1.3 and 1.2 m/s respectively for the test runs with and without tracer gas system. The ambient temperatures were relatively stable at 31.7 °C and 31.3 °C, respectively.

2. Results and discussion

2.1. *Line source experiments*

Scenario 1. Test vehicle only

Fig. 4 shows the variations of CO_2 concentrations measured by roadside air quality sensors under the test vehicle only scenario (i.e., the CO_2 gas is emitted by the test vehicle only). The time starts (i.e., 0 s) when the vehicle head passes by the first pair of sensors (i.e., Sensors #1 and #2 in Fig. 2). The experiments were repeated three times and the plotted curves are the averaged values of the three tests. To ensure data quality, calibrations were carried out before and after the experiments.

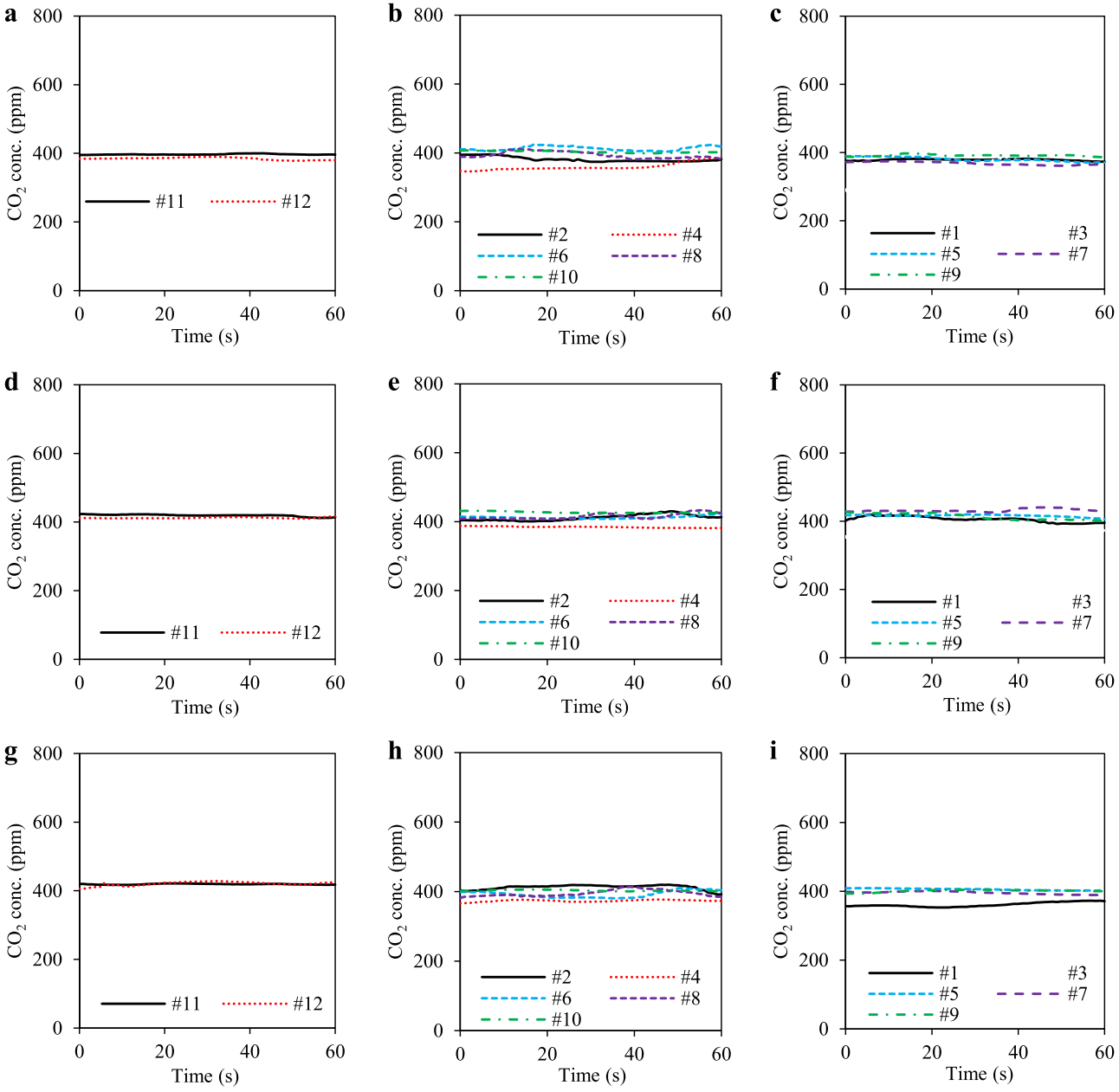

Fig. 4 – Variations of CO_2 concentrations with time measured by roadside air quality sensors under the test vehicle only scenario at various vehicle speeds. (a) 5 km/h - hill side @ 0.8 & 1.6 m; (b) 5 km/h - building side @ 0.8 m; (c) 5 km/h - building side @ 1.6 m; (d) 15 km/h - hill side @ 0.8 & 1.6 m; (e) 15 km/h - building side @ 0.8 m; (f) 15 km/h - building side @ 1.6 m; (g) 30 km/h - hill side @ 0.8 & 1.6 m; (h) 30 km/h - building side @ 0.8 m; (i) 30 km/h - building side @ 1.6 m.

It was confirmed that all sensors were performing within their accuracy specifications, except for one which was malfunctioning (i.e., sensor #3 in Fig. 2 and sensor #1 in Fig. 3). The data from the faulty sensor were omitted in the following analysis and discussion. This data omittance would cause little impact on the analysis or conclusions because only one out of 12 sensors was malfunctioning and other adjacent sensors could compensate the impact. As shown in Fig. 4, there are no obvious concentration spikes when the test vehicle passes by, at either the building or the hill side. In general, all the sensors only measure the background CO_2 concentrations at around 400 ppm. According to the PEMS data, the exhaust mass flow rates of the test vehicle are 0.070, 0.088 and 0.069 kg/s at 5, 15 and 30 km/h, respectively. The corresponding CO_2 concentrations are 2.4 %, 4.1 % and 6.1 %, respectively. Fig. 4 indicates that the exhaust gas produced by test vehicle itself is too small to cause any obvious CO_2 elevations at roadsides, and thus should have insignificant effect on the developed tracer gas system.

Scenario 2. Line source only

Fig. 5 shows the variations of roadside CO_2 concentrations under the line source only scenario (i.e., all CO_2 gas is emitted by the line source system). The time starts when the line source

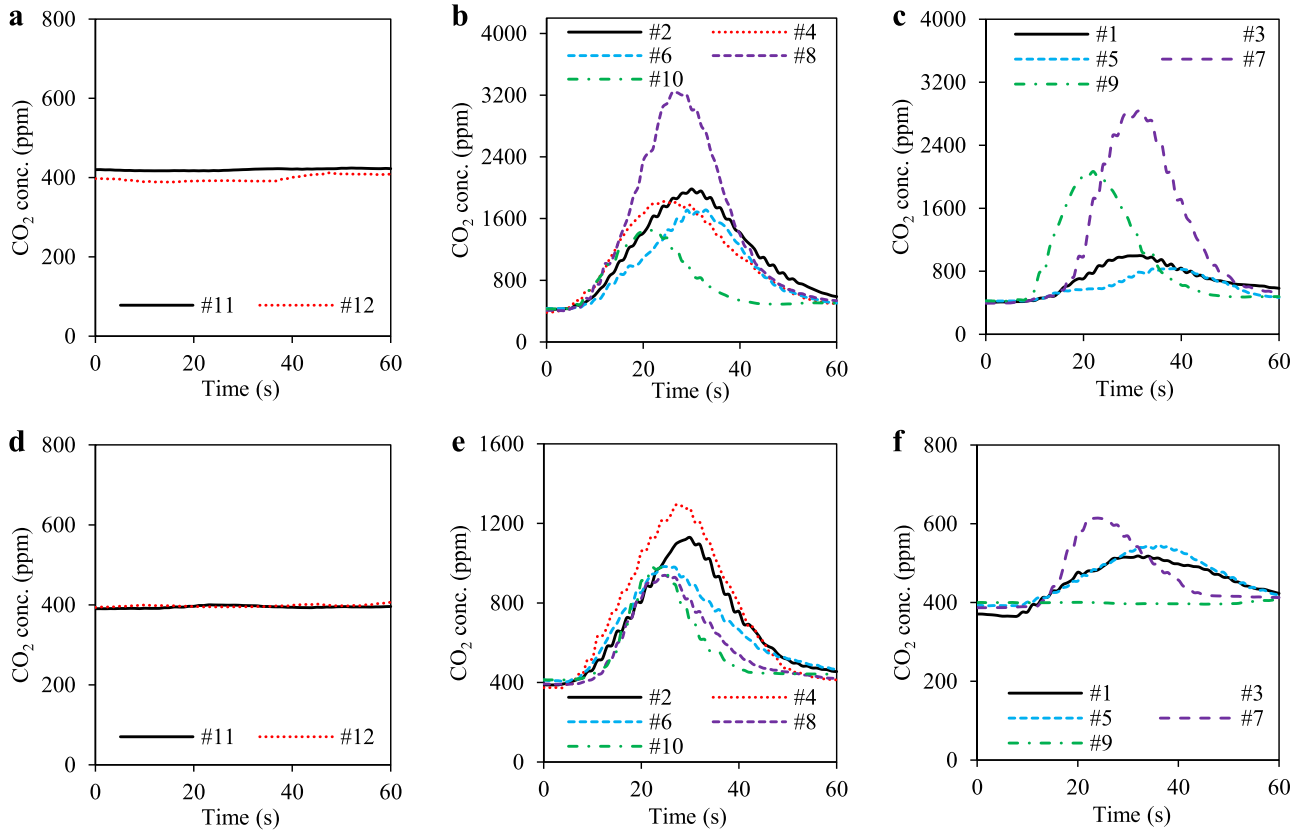

Fig. 5 – Variations of CO_2 concentrations with time measured by roadside air quality sensors under the line source only scenario. (a) High CO_2 release rate - hill side @ 0.8 & 1.6 m; (b) high CO_2 release rate - building side @ 0.8 m; (c) high CO_2 release rate - building side @ 1.6 m; (d) low CO_2 release rate - hill side @ 0.8 & 1.6 m; (e) low CO_2 release rate - building side @ 0.8 m; (f) Low CO_2 release rate - building side @ 1.6 m.

is switched on. The experiments were repeated three times for the high CO_2 release rate condition and four times for the low CO_2 release rate condition. The plotted curves are the averaged values. Comparing with the test vehicle only scenario (Fig. 4), Fig. 5 shows obvious CO_2 elevations at the building side under the line source only scenario due to the much higher CO_2 release rates (i.e., 0.061–0.073 kg/s pure CO_2 gas from the line source vs 0.069–0.088 kg/s exhaust gas with 2.4 %–6.1 % CO_2 from the test vehicle). However, the hill side sensors still could not measure any obvious changes under the line source only scenario. The line source was placed next to the building side sensors (0.3 m, Fig. 2) but far from the hill side sensors (10.9 m, Fig. 2), causing very high CO_2 elevations at the building side but no measurable changes at the hill side. For the same reason, the sensors at 0.8 m height always measured higher CO_2 elevations than those at 1.6 m height. These results imply that, using the current CO_2 release rates, the developed line source system would not be suitable for pollutant dispersion experiments in wide street canyons. The system may likely work for two-lane roads with a divider between the lanes, where the line source can be placed. The line source configuration is a better simulation of the emissions from vehicles on a road in real life. Through the measured data, one can figure out the turbulence induced by vehicle movement in the road section under study, so that an urban canyon emission dispersion model can be developed or validated.

It is also noted that three sensors at 1.6 m (i.e., #1 and #5 in Fig. 5c and #9 in Fig. 5f) recorded obviously lower CO_2 concentrations than their adjacent sensors at the same height. This may be caused by two reasons. First, despite rapid developments in recent years, stability remains a key challenge for low-cost air quality sensors (Castell et al., 2017; Chojer et al., 2020; Kumar et al., 2015; Liu et al., 2020). In this study, pre- and post-calibrations were conducted to confirm that these three sensors were functioning normally. However, the possibility of having gas path leakage in the sensors, which may occur during the transportation or experiments, could not be ruled out. The leakage could cause a lower response in measurements. To address this issue, future studies may deploy more sensors to compensate faulty readings. Second, although these sensors measured relatively low readings in one experiment, they did capture some peaks in other experiments, suggesting that other factors may have caused these unexpected low readings. More specifically, sensors #1 and #9 were placed at the two ends of the canyon and hence may be more vulnerable to changes in ambient wind conditions. Future studies should deploy anemometers to measure the instantaneous wind speeds and directions along with the roadside air quality sensors.

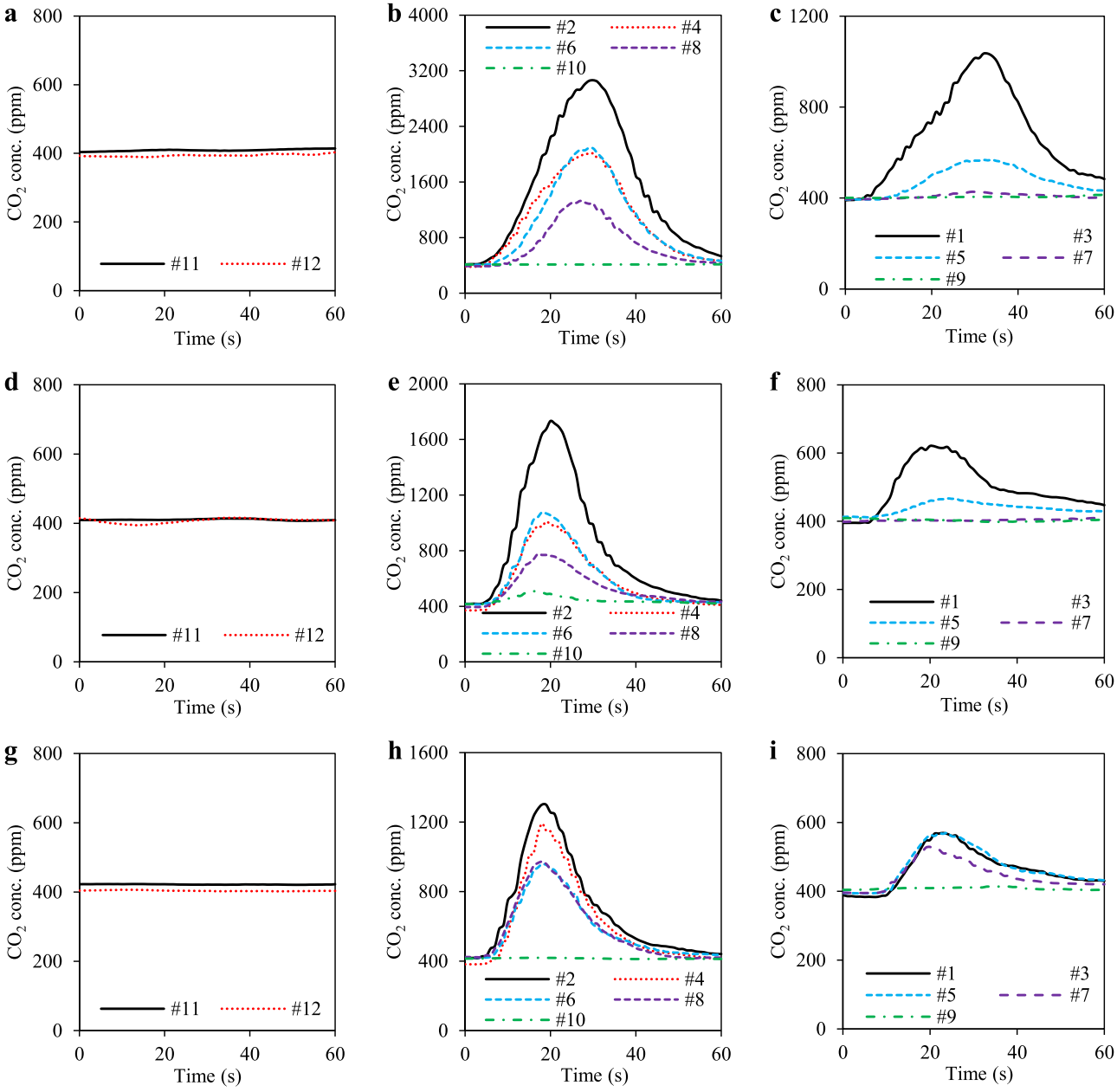

Fig. 6 – Variations of CO_2 concentrations with time measured by roadside air quality sensors under test vehicle plus line source (high CO_2 release rate) scenario at various vehicle speeds. (a) 5 km/h - hill side @ 0.8 & 1.6 m; (b) 5 km/h - building side @ 0.8 m; (c) 5 km/h - building side @ 1.6 m; (d) 15 km/h - hill side @ 0.8 & 1.6 m; (e) 15 km/h - building side @ 0.8 m; (f) 15 km/h - building side @ 1.6 m; (g) 30 km/h - hill side @ 0.8 & 1.6 m; (h) 30 km/h - building side @ 0.8 m; (i) 30 km/h - building side @ 1.6 m.

Fig. 5 also shows that all the CO_2 peak concentrations appear at around 30 s after the line source is switched on. Comparing with the high rate condition (0.073 kg/s), although the CO_2 source rate was only slightly reduced in the low rate condition (0.061 kg/s), the measured roadside CO_2 concentration peak was significantly reduced (~2800 ppm @ 1.6 m and 3200 ppm @ 0.8 m under high rate condition vs ~600 ppm @ 1.6 m and ~1300 ppm @ 0.8 m under low rate condition). This is mainly because the ambient wind speed was higher during the low rate experiments (2.0 m/s) than that during the high rate experiments (0.8 m/s). A higher wind speed results in more dilution and facilitates the mixing and dispersion of exhaust emissions, leading to lower concentrations at roadsides. Normalising the roadside CO_2 concentrations by wind speeds (Gromke and Ruck, 2012) reduces the variations between low and high rates conditions (see **Appendix A Method** and **Fig. S1**).

Scenario 3. Test vehicle plus line source

Figs. 6 and 7 show the effect of vehicle induced turbulence on the emission dispersion process under high and low line source rates conditions, respectively. The time starts when the

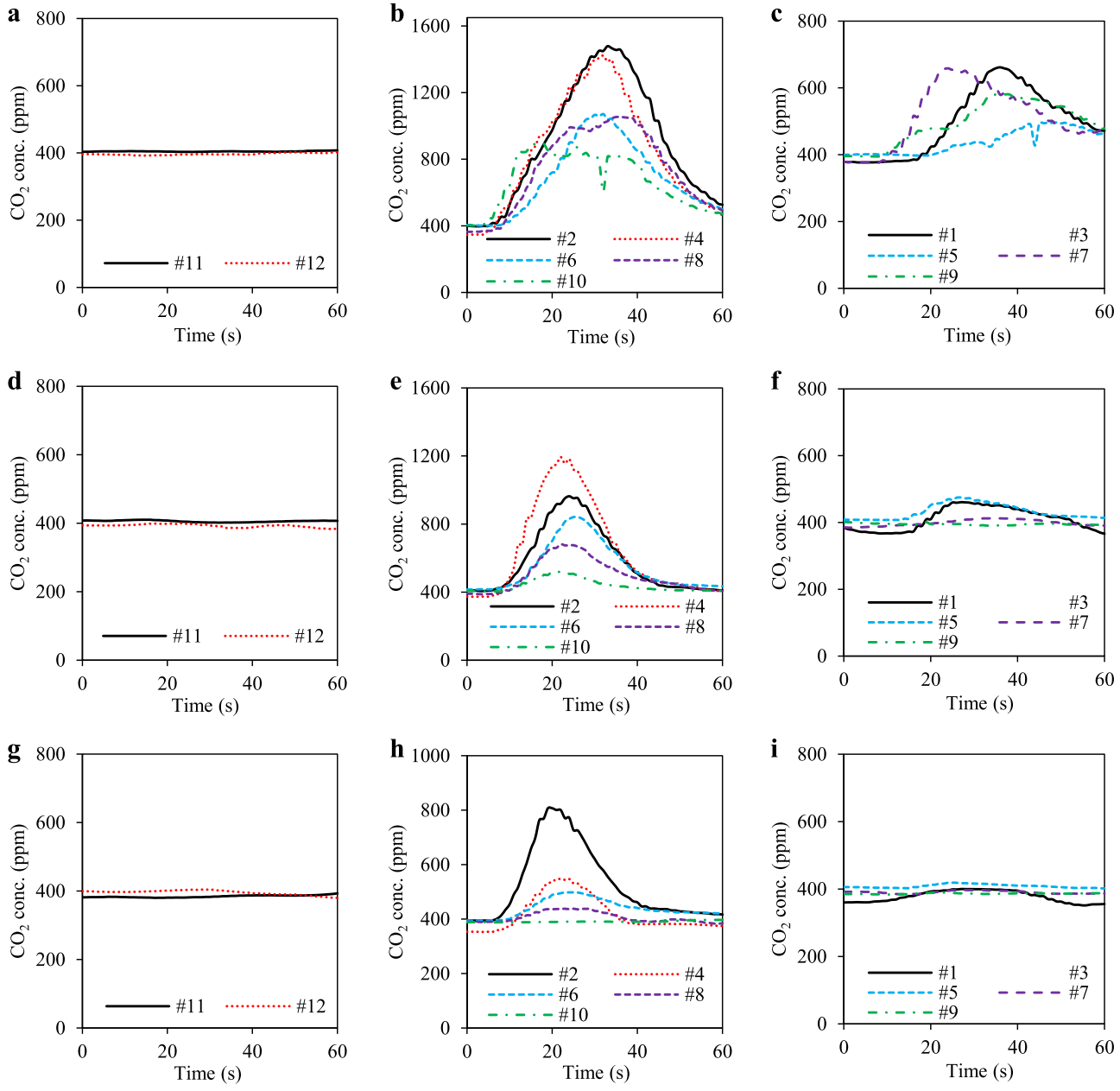

Fig. 7 – Variations of CO_2 concentrations with time measured by roadside air quality sensors under test vehicle plus line source (low CO_2 release rate) scenario at various vehicle speeds. (a) 5 km/h - hill side @ 0.8 & 1.6 m; (b) 5 km/h - building side @ 0.8 m; (c) 5 km/h - building side @ 1.6 m; (d) 15 km/h - hill side @ 0.8 & 1.6 m; (e) 15 km/h - building side @ 0.8 m; (f) 15 km/h - building side @ 1.6 m; (g) 30 km/h - hill side @ 0.8 & 1.6 m; (h) 30 km/h - building side @ 0.8 m; (i) 30 km/h - building side @ 1.6 m.

line source is switched on. All experiments were repeated five times and the plotted curves were the averaged values. Comparing with the line source only scenario (Fig. 5), the moving vehicle facilitates the emission mixing and dispersion processes, especially under high driving speed conditions. This has been clearly demonstrated by the peak CO_2 concentrations and their phases.

Under the line source only (high rate) condition (Fig. 5b-c), the peak CO_2 concentrations are 3200 ppm @ 0.8 m and 2800 ppm @ 1.6 m, with both appearing at ~ 30 s. They are reduced to 3050 ppm @ 0.8 m and 1000 ppm @ 1.6 m, while the phases are unchanged (~30 s) when the vehicle speed is low at 5 km/h (Fig. 6b-c). As the vehicle speed increases, the peak concentrations reduce significantly and their phases advance. When the vehicle speed is increased to 30 km/h, the peak concentrations are only ~1300 ppm @ 0.8 m and ~600 ppm @ 1.6 m, and their phases advance to ~20 s (Fig. 6h-i).

In comparison, the effect of vehicle induced turbulence on emission dispersion is less obvious under low line source rate

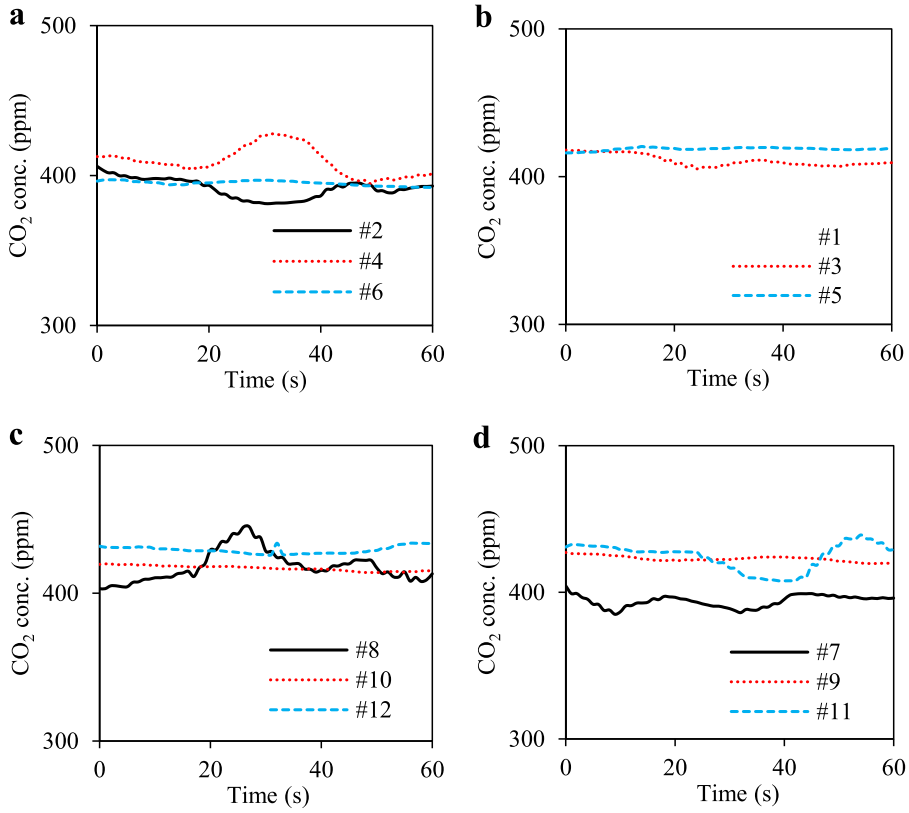

Fig. 8 – Variations of CO_2 concentrations with time measured by individual roadside air quality sensors when point source tracer gas system is off. (a) Building side @ 0.8 m; (b) Building side @ 1.6 m; (c) Hill side @ 0.8 m; (d) Hill side @ 1.6 m.

conditions. Under the line source only (low rate) condition (Fig. 5e-f), the peak CO_2 concentrations are ~1300 ppm @ 0.8 m and 600 ppm @ 1.6 m, which appear at 30 and 25 s, respectively. At a low vehicle speed of 5 km/h (Fig. 7b-c), they are even slightly increased to ~1450 ppm @ 0.8 m and 650 ppm @ 1.6 m, and their phases are delayed to ~35 s. At a higher speed of 30 km/h, the peak concentration is reduced to ~800 ppm at 20 s at the height of 0.8 m, while the CO_2 elevation becomes relatively unobvious at 1.6 m (Fig. 7h-i).

In real-world urban street canyons, vehicle speeds are usually higher than 30 km/h and there are many vehicles passing by continuously, which are expected to greatly enhance the dispersion of vehicle emissions. The results in Figs. 6 and 7 imply that the developed line source tracer gas system is suitable for low speed traffic conditions, but requires a higher line source flow rate if it is used for high speed conditions. Despite the enhancing effect of vehicle induced turbulence on mixing and dispersion of emissions, the hill side sensors still could not measure any CO_2 elevations due to their long distance from the line source. Similar to Fig. 5, we noticed that some sensors (i.e., sensors #7, #9 and #10) captured relatively low readings, probably due to gas path leakage in these sensors and/or changes in ambient winds, as discussed above.

2.2. *Point source experiments*

Fig. 8 shows the variations of CO_2 concentrations measured by individual roadside air quality sensors when the point source tracer gas system is off (i.e., all CO_2 gas is emitted by the test vehicle itself). The time starts when the vehicle head passes by the first pair of sensors (i.e., sensors #1 and #2 in Fig. 3). The experiments were repeated three times and the plotted curves are their averaged values. As shown in Fig. 8, generally, there are no obvious concentration spikes when the test vehicle passes by, for both building and hill sides, and at both 0.8 and 1.6 m heights. In general, all sensors only measure the background CO_2 concentrations at around 400 ppm. This indicates that the exhaust gas from the engine itself would be too small to cause obvious CO_2 elevations at roadsides, and thus should have insignificant effect on the point source tracer gas system.

Fig. 9 shows the variations of CO_2 concentrations measured by individual roadside air quality sensors when the point source tracer gas system is on (i.e., CO_2 gas is emitted by both the test vehicle and tracer gas system). The experiments were repeated five times and the plotted curves were the averaged values. In comparison with the tracer gas off condition (Fig. 8), Fig. 9 shows obvious CO_2 elevations at the building side at about 35 s after the vehicle passes by. The CO_2 elevations are bigger at the 0.8 m than at 1.6 m. However, the sensors at the hill side do not demonstrate any obvious CO_2 elevations.

Nevertheless, Fig. 9, as well as Fig. 8, shows significant differences between individual sensors, which may be caused by signal noises, vibrations, sensor sensitivities and turbulence. Therefore, the CO_2 concentrations measured by the three sensors at the same height (i.e., 0.8 or 1.6 m) and same side (i.e.,

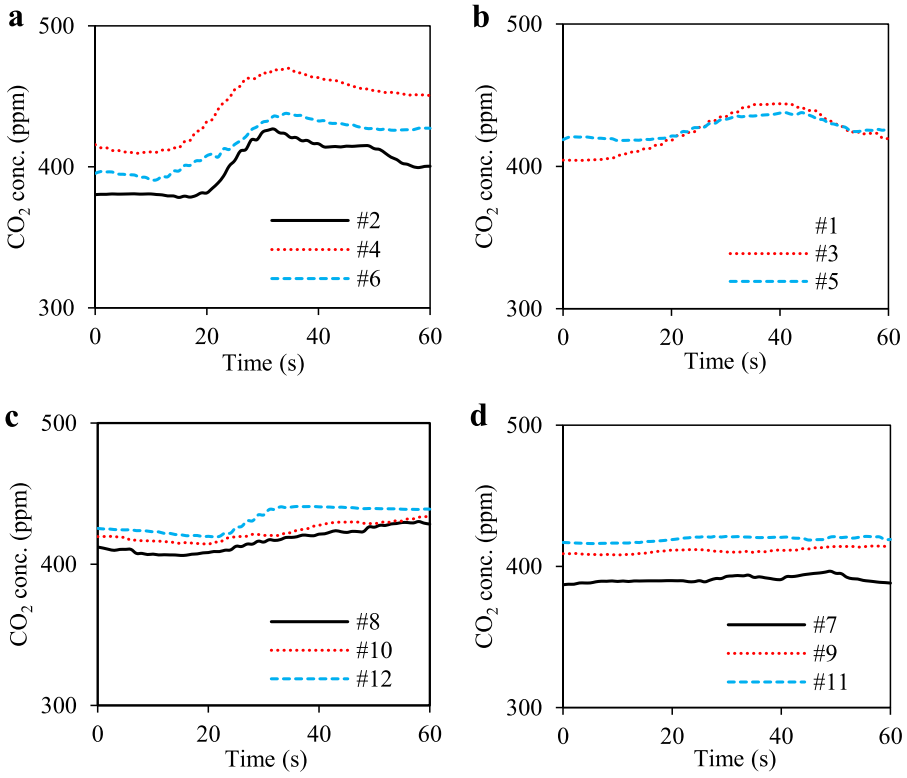

Fig. 9 – Variations of CO_2 concentrations with time measured by individual roadside air quality sensors when the point source tracer gas system is turned on. (a) Building side @ 0.8 m; (b) building side @ 1.6 m; (c) hill side @ 0.8 m; (d) hill side @ 1.6 m.

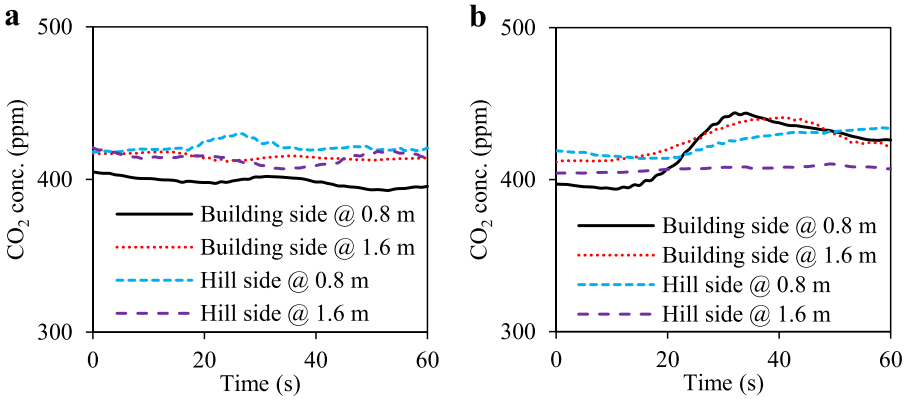

Fig. 10 – Variations of averaged CO_2 concentrations with time. (a) Tracer gas off; (b) tracer gas on.

building or hill) are averaged, by applying a time delay of 1 s based on 4.5 m sensor spacing and 15 km/h vehicle speed. Such averaging is reasonable for point source experiments (but not for line source experiments) because the three sensors are identical to the emission source except for a 4.5 m spacing.

Fig. 10 shows the averaged CO_2 concentrations at each sensor height. When the tracer gas system is off, all roadside CO_2 concentrations are generally unchanged at the background concentration (i.e., ~400 ppm). When the tracer gas system is on, roadside air quality sensors at the building side measure obvious increases in CO_2 concentrations at 30–45 s, while sensors at the hill side do not measure any noticeable changes. In addition, CO_2 elevation is more significant at 0.8 m (50 ppm) than at 1.6 m (40 ppm). This is mainly because the tailpipe exit is at the building side and is at a height closer to 0.8 m, making sensors at 0.8 m on the building side the closest to the tailpipe exit. As a result, exhaust gas has the least dilution when reaching these sensors which consequently record the highest CO_2 increases.

Comparing with the line source experiments at the same vehicle speed (i.e., 600–1700 ppm in Fig. 6e-f and 450-1,200 ppm in Fig. 7e-f), the CO_2 elevations caused by point source (40–50 ppm in Fig. 10) are much lower. This may be due

to two main reasons. Firstly, the point source tracer gas system adopted more connections and valves, leading to much lower CO_2 release rate than the line source system. The PEMS data showed that the point source tracer gas system only released about 0.010 kg/s of pure CO_2 gas into the tailpipe of the test vehicle, which was over 80 % lower than that of the line source system (i.e., 0.061–0.073 kg/s of pure CO_2 gas). Secondly, the point source was farther to the building side sensors (Fig. 3) than the line source (Fig. 2), leading to greater dispersion when reaching the sensors.

3. Conclusions, limitations and recommendations

3.1. *Conclusions*

This study investigated the feasibility of using CO_2 as a tracer gas for characterising the dispersion process of vehicle emissions in a real-world street canyon. The experimental data showed unmeasurable CO_2 concentration changes when the test vehicle passed by without the tracer gas system, indicating that the CO_2 gas generated by the test vehicle itself had an insignificant effect. When the tracer gas system was on (for both line and point sources), the roadside air quality sensors on the building side measured noticeable CO_2 elevations, while the hill side sensors did not. In addition, the measured CO_2 elevations were larger at 0.8 m than that at 1.6 m.

To make CO_2 a suitable tracer gas for studying air pollutant dispersion in an urban street canyon, the benchmark should be whether one can use a practicable amount of the gas (i.e., CO_2) to adequately characterize air pollutant dispersion. The "practicable amount of the gas" centres on two considerations. One is whether the consumption of the gas is "affordable", which is to be judged more or less by common sense in terms of cost, safety and health concerns. The other is whether the supply and distribution of the gas can be "conveniently set up in-situ", particularly at roadside. These are practical considerations. To "adequately characterize" the air pollutant dispersion, the resulting changes in the ambient concentration of the gas at the study location should be of a magnitude sufficient for quantifying the dispersion characteristics for dispersion model development or validation, even though there are other sources of the gas in the measurement locality such as the co-existing vehicles.

The experimental data presented in this study demonstrate that the employed CO_2 tracer gas system (both point and line sources) is suitable for characterising emission dispersion under controlled conditions (i.e., one lane, one vehicle), which provides very important data for the development and verification of CFD and Gaussian dispersion models.

3.2. *Limitations*

However, when it comes to real world situation in which there are many vehicles and the line source is placed at road centre (e.g., 1–2 lanes in each direction), the CO_2 changes at roadside may be very small or unmeasurable, unless the line source has a sufficiently high emission rate. This is evidenced by our experimental data since the building side sensors measured high concentrations (0.3 and ~5 m away from line and point sources, respectively), while the hill side sensors measured no CO_2 changes (~10 and ~5 m away from line and point sources, respectively). This is mainly because the current tracer gas system could not release sufficient CO_2 (limited by the valve and condensation). The CO_2 release rate in the present experiments was up to 0.073 kg/s for no more than 20 s (i.e., <1.5 kg of CO_2 per experiment). A bigger tracer gas system will still be affordable, if used for a larger street canyon and placed at road centre.

3.3. *Recommendations*

Overall, our field experiments demonstrated that using CO_2 as a tracer gas is feasible for investigating vehicle emission dispersion in real-world street canyons. For future field experiments, a higher CO_2 release rate is recommended and the developed method is more suitable for small street canyons (e.g., single- or double-lane streets with low traffic volumes). It is worth noting that this pilot study was preliminary and was not conducted in a typical street canyon as one side of the road was a steep hill. Future studies should be conducted in a real-world urban street canyon to further verify the feasibility of CO_2 as a tracer gas for characterising vehicle emission dispersion. Furthermore, although experiments were performed in relatively calm days, wind conditions were measured using low-grade devices and hence were paid little attention in the present analysis. Future studies will need to more accurately characterise instantaneous wind speeds and directions to enable an adequate normalisation of concentration data. Finally, the stability of low-cost sensors remains a challenge. Future studies should adopt more sensors to form a higher resolution sensors network for more reliable statistics and adopt more accurate and reliable sensors if available.

Declaration of competing interest

The authors declare that they have no known competing financial interests or personal relationships that could have appeared to influence the work reported in this paper.

CRediT authorship contribution statement

Yuhan Huang: Writing – review & editing, Writing – original draft, Funding acquisition, Formal analysis. **Helen B. Wang:** Writing – review & editing, Investigation, Funding acquisition. **Hilda M.W. Mak:** Writing – review & editing, Investigation. **Mengyuan Chu:** Writing – review & editing, Investigation. **Zhi Ning:** Writing – review & editing, Funding acquisition. **Bruce Organ:** Writing – review & editing, Investigation. **Edward F.C. Chan:** Writing – review & editing, Funding acquisition. **Chun-Ho Liu:** Writing – review & editing, Funding acquisition. **Wai-Chuen Mok:** Writing – review & editing, Funding acquisition. **Christof Gromke:** Writing – review & editing. **Ho Kyong Shon:** Writing – review & editing. **Chengwang Lei:** Writing – review & editing, Supervision. **John L. Zhou:** Writing – review & editing, Supervision.

Acknowledgements

This work was supported by the Environment and Conservation Fund (No. ECF 14/2018) of the Hong Kong SAR Government, China. Dr Yuhan Huang is a recipient of the ARC Discovery Early Career Research Award (DE220100552).

Appendix A Supplementary data

Supplementary material associated with this article can be found in the online version at doi:10.1016/j.jes.2024.06.036.

References

Alexeeff, S.E., Roy, A., Shan, J., Liu, X., Messier, K., Apte, J.S., et al., 2018. High-resolution mapping of traffic related air pollution with Google street view cars and incidence of cardiovascular events within neighborhoods in Oakland. CA. Environ. Health 17, 38.

Brimblecombe, P., Chu, M.-Y., Liu, C.-H., Ning, Z., 2021. NO_x and CO fluctuations in a busy street canyon. Environments 8, 137.

Casquero-Vera, J.A., Lyamani, H., Titos, G., Borrás, E., Olmo, F.J., Alados-Arboledas, L., 2019. Impact of primary NO_2 emissions at different urban sites exceeding the European NO_2 standard limit. Sci. Total Environ. 646, 1117–1125.

Castell, N., Dauge, F.R., Schneider, P., Vogt, M., Lerner, U., Fishbain, B., et al., 2017. Can commercial low-cost sensor platforms contribute to air quality monitoring and exposure estimates? Environ. Int. 99, 293–302.

Cheng, J., Ho, H.C., Webster, C., Su, H., Pan, H., Zheng, H., et al., 2021. Lower-than-standard particulate matter air pollution reduced life expectancy in Hong Kong: a time-series analysis of 8.5 million years of life lost. Chemosphere 272, 129926.

Chojer, H., Branco, P.T.B.S., Martins, F.G., Alvim-Ferraz, M.C.M., Sousa, S.I.V., 2020. Development of low-cost indoor air quality monitoring devices: recent advancements. Sci. Total Environ. 727, 138385.

Chu, M., Brimblecombe, P., Wei, P., Liu, C.-H., Du, X., Sun, Y., et al., 2022. Kerbside NO_x and CO concentrations and emission factors of vehicles on a busy road. Atmos. Environ. 271, 118878.

Connan, O., Leroy, C., Derkx, F., Maro, D., Hébert, D., Roupsard, P., et al., 2011. Atmospheric dispersion of an elevated release in a rural environment: comparison between field SF6 tracer measurements and computations of Briggs and ADMS models. Atmos. Environ. 45, 7174–7183.

Fu, L., Yang, M., Niu, J., Ren, W., You, R., 2022. Transient tracer gas measurements: development and evaluation of a fast-response SF6 measuring system based on quartz-enhanced photoacoustic spectroscopy. Indoor Air 32, e12952.

Grange, S.K., Lewis, A.C., Moller, S.J., Carslaw, D.C., 2017. Lower vehicular primary emissions of NO2 in Europe than assumed in policy projections. Nat. Geosci. 10, 914–918.

Gromke, C., Jamarkattel, N., Ruck, B., 2016. Influence of roadside hedgerows on air quality in urban street canyons. Atmos. Environ. 139, 75–86.

Gromke, C., Ruck, B., 2012. Pollutant concentrations in street canyons of different aspect ratio with avenues of trees for various wind directions. Boundary-Layer Meteorol 144, 41–64.

Guo, Z., Mosley, R.B., Wasson, S.J., Fortmann, R.C., McBrian, J.A., 2001. Dissociation of Sulfur Hexafluoride Tracer Gas in the Presence of an Indoor Combustion Source. J. Air Waste Manag. Assoc. 51, 616–622.

Harrison, J.J., 2020. New infrared absorption cross sections for the infrared limb sounding of sulfur hexafluoride (SF6). J. Quant. Spectrosc. Radiat. Transf. 254, 107202.

Hedley Environmental Index, 2023. Historical Data. School of Public Health of The University of Hong Kong Available:. https://hedleyindex.hku.hk/en/historical-data# Accessed July 20, 2023.

Hossain, M.S., Frey, H.C., Louie, P.K.K., Lau, A.K.H., 2021. Combined effects of increased O_3 and reduced NO_2 concentrations on short-term air pollution health risks in Hong Kong. Environ. Pollut. 270, 116280.

Huang, X.-T., Huang, Y.-D., Xu, N., Luo, Y., Cui, P.-Y., 2020a. Thermal effects on the dispersion of rooftop stack emission in the wake of a tall building within suburban areas by wind-tunnel experiments. J. Wind Eng. Ind. Aerod. 205, 104295.

Huang, Y., Lee, C.K.C., Yam, Y.-S., Mok, W.-C., Zhou, J.L., Zhuang, Y., et al., 2022. Rapid detection of high-emitting vehicles by on-road remote sensing technology improves urban air quality. Sci. Adv. 8, eabl7575.

Huang, Y., Lei, C., Liu, C.-H., Perez, P., Forehead, H., Kong, S., et al., 2021. A review of strategies for mitigating roadside air pollution in urban street canyons. Environ. Pollut. 280, 116971.

Huang, Y., Mok, W.-c., Yam, Y.-s., Zhou, J.L., Surawski, N.C., Organ, B., et al., 2020b. Evaluating in-use vehicle emissions using air quality monitoring stations and on-road remote sensing systems. Sci. Total Environ. 740, 139868.

Kumar, P., Morawska, L., Martani, C., Biskos, G., Neophytou, M., Di Sabatino, S., et al., 2015. The rise of low-cost sensing for managing air pollution in cities. Environ. Int. 75, 199–205.

Kwok, Y.T., Schoetter, R., de Munck, C., Lau, K.K.-L., Wong, M.S., Ng, E., 2021. High-resolution mesoscale simulation of the microclimatic effects of urban development in the past, present, and future Hong Kong. Urban Clim 37, 100850.

Laporthe, S., Virgone, J., Castanet, S., 2001. A comparative study of two tracer gases: SF_6 and N_2O. Build. Environ. 36, 313–320 .

Lee, C., 2019. Impacts of urban form on air quality: emissions on the road and concentrations in the US metropolitan areas. J. Environ. Manage. 246, 192–202.

Li, F., Zhou, T., 2019. Effects of urban form on air quality in China: an analysis based on the spatial autoregressive model. Cities 89, 130–140.

Li, Y., Zhang, X., Zhang, J., Xiao, S., Xie, B., Chen, D., et al., 2019. Assessment on the toxicity and application risk of C_4F_7N: a new SF_6 alternative gas. J. Hazard. Mater. 368, 653–660.

Liu, X., Jayaratne, R., Thai, P., Kuhn, T., Zing, I., Christensen, B., et al., 2020. Low-cost sensors as an alternative for long-term air quality monitoring. Environ. Res. 185, 109438.

Mendes, L.B., Edouard, N., Ogink, N.W.M., van Dooren, H.J.C., Tinôco, I.d.F.F., Mosquera, J., 2015. Spatial variability of mixing ratios of ammonia and tracer gases in a naturally ventilated dairy cow barn. Biosyst. Eng. 129, 360–369.

Pettit, T., Torpy, F.R., Surawski, N.C., Fleck, R., Irga, P.J., 2021. Effective reduction of roadside air pollution with botanical biofiltration. J. Hazard. Mater. 414, 125566.

Rivas, E., Santiago, J.L., Lechón, Y., Martín, F., Ariño, A., Pons, J.J., et al., 2019. CFD modelling of air quality in Pamplona City (Spain): assessment, stations spatial representativeness and health impacts valuation. Sci. Total Environ. 649, 1362–1380.

Simmonds, P.G., Palmer, P.I., Rigby, M., McCulloch, A., O'Doherty, S., Manning, A.J., 2021. Tracers for evaluating computational models of atmospheric transport and oxidation at regional to global scales. Atmos. Environ. 246, 118074.

Takekawa, H., Chatani, S., Ito, A., 2013. A new approach for estimation of the effect of NOx emission reduction on roadside NO_2 concentration in Tokyo. Atmos. Environ. 68, 92–102.

Tan, W., Li, C., Wang, K., Zhu, G., Liu, L., 2019. Geometric effect of buildings on the dispersion of carbon dioxide cloud in

idealized urban street canyons. Process Saf. Environ. Prot. 122, 271–280.
Tan, W., Li, C., Wang, K., Zhu, G., Wang, Y., Liu, L., 2018. Dispersion of carbon dioxide plume in street canyons. Process Saf. Environ. Prot. 116, 235–242.
Wu, X., Vu, T.V., Harrison, R.M., Yan, J., Hu, X., Cui, Y., et al., 2022. Long-term characterization of roadside air pollutants in urban Beijing and associated public health implications. Environ. Res. 212, 113277.
Xu, G., Luxbacher, K.D., Ragab, S., Schafrik, S., 2013. Development of a remote analysis method for underground ventilation systems using tracer gas and CFD in a simplified laboratory apparatus. Tunn. Undergr. Space Technol. 33, 1–11.
Yang, J., Shi, B., Zheng, Y., Shi, Y., Xia, G., 2020. Urban form and air pollution disperse: key indexes and mitigation strategies. Sustain. Cities Soc. 57, 101955.
Zhang, Q., Zhang, X., Ye, W., Zhi, C., Huang, Y., Gao, J., 2022. Transport characteristics of dense gaseous contaminants in a large space in the presence of obstacles. Build. Environ. 207, 108411.
Zheng, Y., Ren, C., Xu, Y., Wang, R., Ho, J., Lau, K., et al., 2018. GIS-based mapping of Local Climate Zone in the high-density city of Hong Kong. Urban Clim 24, 419–448.
Zhou, S., Lin, R., 2019. Spatial-temporal heterogeneity of air pollution: the relationship between built environment and on-road PM2.5 at micro scale. Transp. Res. Part D 76, 305–322.